Proceedings of the ASME 2010 Conference on Smart Materials, Adaptive Structures and Intelligent Systems
SMASIS2010
September 28 – October 1, 2010, Philadelphia, Pennsylvania, USA

SMASIS2010-3689
DRAFT

ENERGY SCAVENGING COMBINING PIEZOELECTRIC AND PYROELECTRIC EFFECTS

Ugur Erturun Rachel Waxman Christopher Green
Matthew Lee Richeson Karla Mossi
Department of Mechanical Engineering, Virginia Commonwealth University, Richmond, VA, USA

ABSTRACT

The piezoelectric effect is well known and used for vibration energy harvesting applications. The pyroelectric effect is also used to generate electrical power if there is an environment that has cyclic temperature changes. In this study, increasing generated electrical power by use of a combination of piezoelectric and pyroelectric effects is investigated. As a sample case it is aimed to utilize this piezoelectric and pyroelectric effect for a new sensor application. The results of the tests indicate that energy from vibrations and heat can have a significant interaction depending on the frequencies at which each effect occurs. In some cases, energy from vibrations and energy from heat can be detrimental when combined. Therefore both parameters have to be tuned properly to optimize scavenging energy. It was determined that at the best tested parameters the rate of charge increases by approximately 12%.

INTRODUCTION

Renewable and alternative energy sources have been moved to the forefront of research and development to reduce the world's dependence on petroleum products. Efforts are being made to design systems that capture energy being lost to the ambient environment. Energy can be reclaimed through a process and stored for later use to recharge a battery or power a device. This process is referred to as energy scavenging with the general idea being the extraction of energy that would otherwise be wasted. Energy sources that are frequently squandered include solar, wind, water, indoor lighting, vibrations, acoustic noise, and temperature gradients. Others include the energy generated by humans from everyday activities such as walking, driving, or sleeping [1]. Harvesting these phenomena can be accomplished through the use of piezoelectric and pyroelectric materials such as lead ziconate titanate (PZT), lead magnesium niobate-lead titanate (PMN-PT), and polyvinylidene fluoride (PVDF).

Piezoelectric Energy Conversion

Piezoelectricity describes the phenomenon of generating an electric charge in a material when subjecting it to mechanical stress (direct effect), and conversely, generating a mechanical strain in response to an applied electric field (converse effect). The effects are practically linear as the electric field and mechanical strain are proportional. This characteristic allows a material to be used as a sensor and an actuator [2]. The equations that describe the behavior of piezoelectric materials are given usually by their constitutive equations in tensor notation, which can be written as:

$$D_i = \varepsilon_{ij} E_j + d_{ijk} T_{jk} \qquad (1)$$

And

$$S_{ij} = d_{ijk} E_k + s^E_{ijkl} T_{kl} \qquad (2)$$

Where T is stress, E is electric field, D is displacement, S is strain, s is compliance, d is strain constant, and ε is permittivity.

Several studies have investigated the possibility of harvesting energy through the use of piezoelectric materials (which are also pyroelectric) [3], [4], [5], [6]. Goldfarb and Umeda measured the power and calculated the efficiency of an output produced by a piezoelectric Unimorph, which consists of a layer of piezoelectric material bonded to a piece of metal [7], [8]. Though the efficiency obtained was quite low, their work demonstrated the possibility of using a piezoelectric device to harvest mechanical energy. Antaki et al. explored the

feasibility of extracting energy from ambulation to provide supplemental power to operate artificial organs. Their study measured energy utilized when walking or jogging by the use of piezoelectric stacks [4].

Roundy et al. explored the possibility of scavenging low-level vibrations as a power source for wireless sensor nodes. The optimized model produced energy densities of 250$\mu W/cm^3$ from a vibration source input magnitude of 2.5 m/s^2 at 120 Hz. The model was verified experimentally demonstrating a power density of 70$\mu W/cm^3$ [9].

Sodano, Lloyd, and Inman compared the ability of three types of strain-type actuators, a Macro-Fiber Composite (*MFC*) actuator, the Quick Pack *IDE* model QP10ni, and the Quick Pack model QP10n to convert mechanical strain into electrical energy by exciting them while attached to an aluminum beam. An important concept from this study is that impedance matching between the transducer and the circuit is critical when optimizing for power [10].

Pyroelectric Energy Conversion

Thermoelectric power generation is based on Seebeck effect, which was discovered in 1821. When a temperature difference exists between the two points of the open circuit that is made up of two heterogeneous semiconductors, thermal electromotive force is produced, which is in direct proportion to the temperature difference between the two points. Commercially available thermoelectric generator modules (TGM) can provide on the order of $10mW/cm^2$ [11]. This level of performance comes with difficulty because of the need of bulky heat sinks to maximize the gradient. Pyroelectric materials are an alternative because of their ease of use [12].

Pyroelectricity is based on a pronounced temperature dependence of the electric displacement field in a ferroelectric material. The pyroelectric effect has not been considered for thermal power generation so far perhaps because the electric current generated by pyroelectric effect is proportional to the time derivative of temperature.

Olsen et al. designed a cyclic pyroelectric conversion device using a pump, a cooling system, and a heat exchanger. A DC voltage source and a series of circuits were used to drive a Lead Zirconate plate doped with T^{4+} and Sn^{4+}. The circuit mimicked the behavior of an Ericsson cycle yielding an energy density of $100mJ/cm^3$ [13]. In another study PZT cells of 60µm-100µm were fabricated by Cuadras et al. Poling fields of 5V/µm and 7V/µm were used for each. The samples were heated with a halogen lamp and a hair dryer. It was concluded that the samples with the larger thicknesses had the greater energy densities [14].

Sebald et al. analyzed pyroelectric behavior in terms of thermodynamic cycles with energy harvesting circuitry. An electro-thermal coupling factor was defined and it was concluded that that efficiencies from 0.02% and 0.05%of the Carnot cycle could be reached using (111) PMN-0.25PT and a Synchronized Switch on Inductor (SSHI) circuit [15]. In a later study by the same group, which compared thermoelectric and pyroelectric energy harvesting, it was concluded that pyroelectric energy harvesters were more efficient and easier to implement than traditional thermoelectric materials [16]. Sebald et al. conducted another study the same year and concluded that using an Ericsson based thermodynamic cycle produced 100 times more energy than the linear pyroelectric effect. Materials with high electro-caloric activity were needed for top performance. Energy densities of $186mJ/cm^3$ were reported [17].

Energy Harvesting Circuitry

The type of circuitry used to harvest energy is determined by the desired output to the load, which frequently needs to be rectified, filtered, and regulated. The output signal from the transducer can be modeled as an AC source in parallel with a capacitor. To convert this signal into a useful one, an AC-DC converter is used to rectify the noisy AC signal. The output from this converter is then sent to a DC-DC converter where it is regulated to the desired voltage. Capacitors are used to aid in filtering. Step down buck converters have been receiving widespread use because of their efficiency [18]. They consist of a diode in series with an inductor all in parallel with a capacitor with the switching of the rectified signal being accomplished by a MOSFET [19].

Because of the wide range of energy harvesting circuits available, in this study the circuitry is kept constant. Since the main objective of this study is not to optimize circuitry but to characterize the contributions of the pyroelectric and piezoelectric effect on PZT5A, a commercially available circuitry is utilized. Details of the experimental setup are described in the following section.

EXPERIMENTAL SETUP

In this study, it has been hypothesized that by utilizing both piezoelectric and pyroelectric effects simultaneously, it may be possible to harvest more energy than by utilizing only one effect at a time. To test this, an experimental setup was designed. A PZT sample with dimensions 28.1mm x 28.4mm x 0.375mm was obtained and taped to an aluminum substrate of dimensions 50mm x 150mm x 0.275mm. An M-8503-P1 Macro Fiber Composite (MFC) shown in Figure 1, a commercially available piezoelectric actuator from Smart Material Corporation was taped to the opposite side of the aluminum and was used to provide the vibration input to the PZT sample [20]. It was necessary to power the MFC using a Trek PZD2000 High Voltage Amplifier, which was connected to a HP 33120A Function Generator.

To provide the fluctuating temperature input to the PZT sample, a 125W infrared heating lamp was used as the heat source. A 27.94 cm diameter steel disc was constructed and a 45º sector of the disc was cut away. This disc was fixed to a variable speed DC electrical motor and positioned so that the disc came between the infrared lamp and the test sample. As the disc spun, the test sample was subjected to heat from the lamp for 1/8 of the disc's spin period. It was positioned in such

a way that the aluminum substrate was clamped at one end and the PZT sample was at the free end and directly in front of the lamp. The DC motor received power from a Tenma 72-6615 DC Power Supply. The voltage was adjusted from 0 to 20V in order to spin the disc at different speeds, thus providing different temperature fluctuation frequencies. This experimental setup is depicted as 3D model in Figure 2a. The main dimensions of the experimental setup are shown in Figure 2b.

In order to quantify the power generated by the sample, a Tektronix TDS 2024 oscilloscope was used to measure the voltage waveforms produced by the PZT. It was also used to monitor the input waveforms to the MFC from the function generator and signal amplifier. In addition, a thermocouple was attached to the PZT sample to observe its temperature. An Analog Devices AD595 Thermocouple Amplifier was used to convert the thermocouple signal into one strong enough to be monitored by the oscilloscope. A commercially available energy harvesting circuit, Advanced Linear Devices EH301, was connected directly to the electrodes of the PZT sample. This device automatically matches impedance with its source and rectifies the input signal before storing the charge on an onboard capacitor. The device is designed to charge until the capacitor voltage reaches a high cutoff voltage and then discharge through another powered device until it reaches a low cutoff voltage, at which point it begins charging again. To monitor the capacitor voltage of this device, a Fluke 189 True RMS Multimeter was used. LabVIEW was used to import data from the oscilloscope and FlukeView was used to import data from the multimeter. Data processing diagram of the experimental setup is shown in Figure 3.

The EH301 energy harvesting device that is manufactured by Advanced Linear Devices was used to collect the vibrational and thermal energy from the PZT patch. The module contains electrically programmable analog device (EPAD) MOSFET transistors with programmable voltage thresholds. The two supply threshold voltages for the EH301 are 3.1V for +V_low_DC and 5.2V for +V_high DC correspond to the minimum (V_L) and the maximum voltage (V_H) for the intended application. The module rectifies input voltages while a bank of capacitors handles the storage. An internal circuit monitors the charging of the capacitors until V_H is reached; at that time the output is enabled and it is ready to supply power to an application. The charging waveform of the module is shown in Figure 4 [21].

The independent parameters that were controlled were the vibration frequency and the temperature fluctuation frequency. The amplitude of the signal output by the amplifier to the MFC was always 800Vpp and the infrared lamp was always a set distance (80mm) from the test sample. Four vibration frequencies were tested, three of which were resonance frequencies and one of which was fixed. Because the resonance frequencies of the sample changed depending on its temperature, these frequencies had to be determined by trial and error for each test.

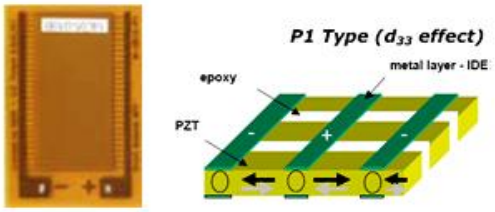

Figure 1. MFC actuator M-8503-P1 [20].

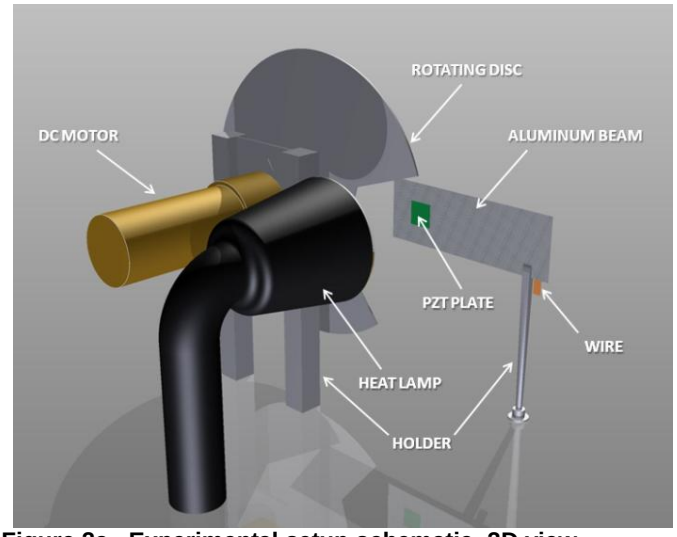

Figure 2a. Experimental setup schematic: 3D view.

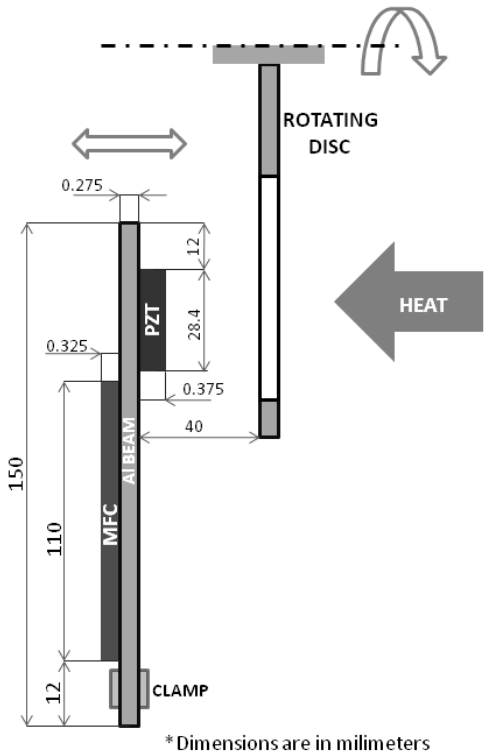

Figure 2b. Experimental setup schematic: 2D view.

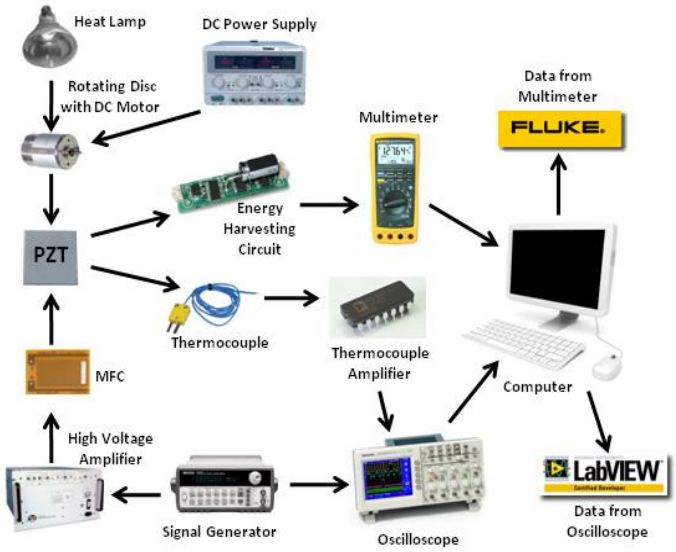

Figure 3. Data processing schematic of the setup.

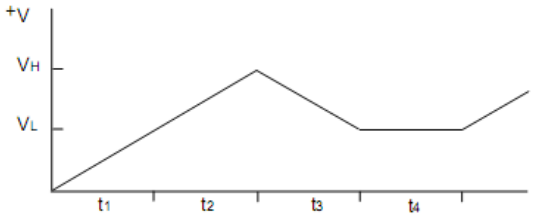

Figure 4. EH301 Charging Wave Form [21].

The resonant frequencies were chosen to be approximately 40Hz, 600Hz, and 900Hz, and the fixed frequency was 500Hz. The temperature fluctuation frequencies were approximately 0.1Hz, 0.5Hz, and 1Hz. Tests were conducted for every combination of these frequencies, including 0Hz, to test the independent contributions of vibration and temperature fluctuations alone. For each test, waveforms were collected by the oscilloscope. The primary measure of power generated was the amount of power harvested by the energy harvesting circuit. Before each test the capacitor on the circuit was shorted. It was then allowed to charge for 30min. The amount of energy harvested on the 1mF capacitor could then be easily calculated by $E = (1/2)CV^2$ where C is the capacitance and V is the measured voltage at 30min. Average power could then be calculated by dividing this number by 1800sec.

RESULTS AND DISCUSSION

The first step of the results consists of measuring temperature profiles as the disk rotates at different speeds. The trends observed in Figures 5a through 5c of temperature versus time show the signals are quite noisy, and to help characterize waveform shape a smoothed version of the data is also shown. Note that the temperature profile with the most scatter is Figure 5c, that is when the frequency of the plate rotating is approximately 1Hz and the plate is rotating relatively quickly. In this case, the samples do not have enough time to cool completely between each cycle and the temperature gradients are small (approximately a ΔT of 1.7°C, which is four times smaller than the 0.1Hz case).

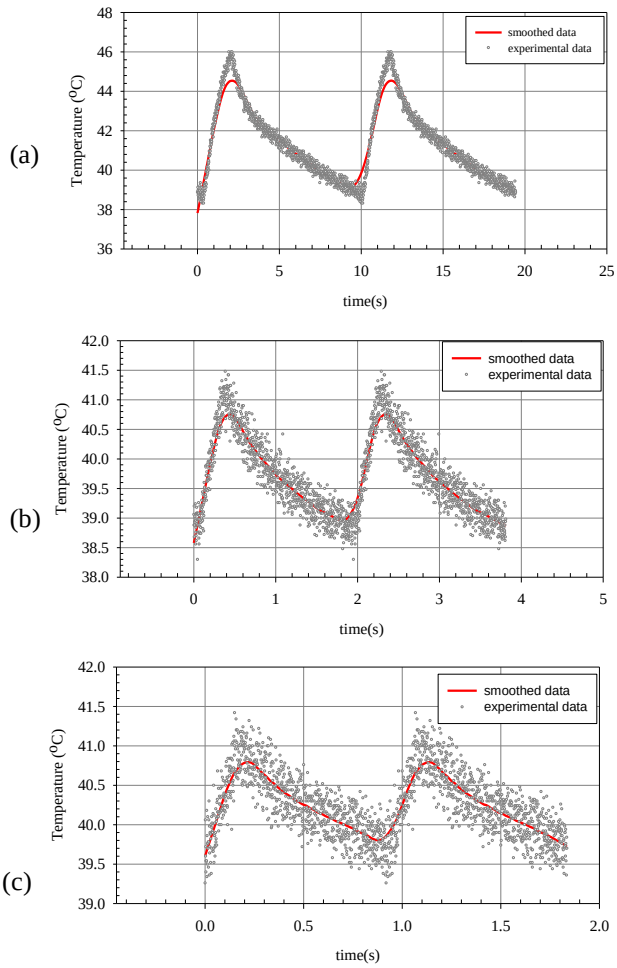

Figure 5. Temperature profiles at (a) 0.1Hz, (b) 0.5Hz (c) 1Hz.

For the case of only providing heat energy to the sample, a typical one-cycle profile is measured as shown in Figure 6 at the three different frequencies tested. The maximum amount of voltage harvested is similar in all cases except for the 1Hz case, which is slightly smaller. The difference is in the area under each curve. This translates to lower total energy that can be harvested. In addition, it is important to note that the values of voltage in the cooling phase reach values below those measured at the initial time. These changes are possible due to the different slopes of the temperature profiles when heating and cooling.

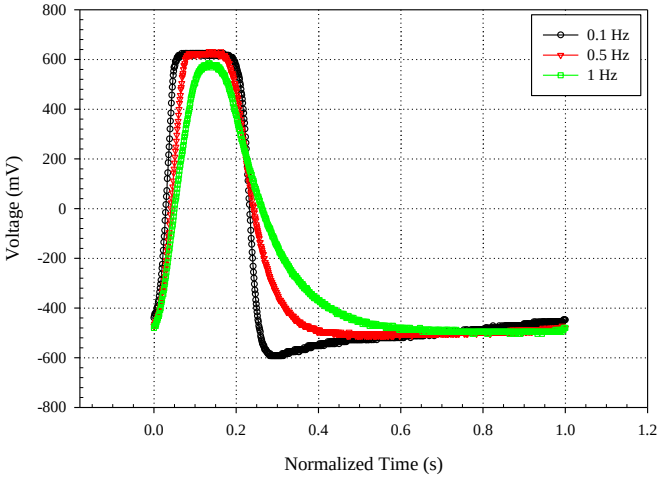

Figure 6. Energy Scavenged through the application of periodic light bursts at different rates.

Using the setup described in the experimental section, a periodic vibration is applied to the beam at different frequencies. In this case the light is turned off, effectively showing voltage profiles when only vibration is present in the system, as shown in Figure 7. The frequencies shown are sample values chosen due to their higher output and quality of the signal.

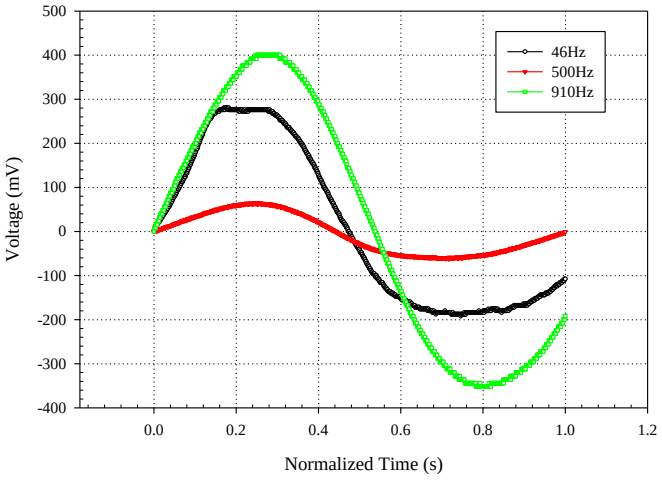

Figure 7. Vibration only Voltage waveforms at different frequencies.

The results shown in Figures 6 and 7 are typical for vibration only and heat only cases. Discussions on power and energy calculations are described later in this section.

When heat and vibration are combined, each one at different setting, the results for each case are different and are described separately. For the case of heat at 0.5Hz and vibration levels of 43, 500, and 620Hz, the typical output waveform of measured voltage is shown in Figure 8.

For instance in the case of applied heat at 0.5Hz and vibrations at 620Hz, the experimental data and smoothed data are displayed in Figure 8. It is hypothesized that the apparent noise is energy coming from applying the cycling heat signal simultaneously with the applied vibrations.

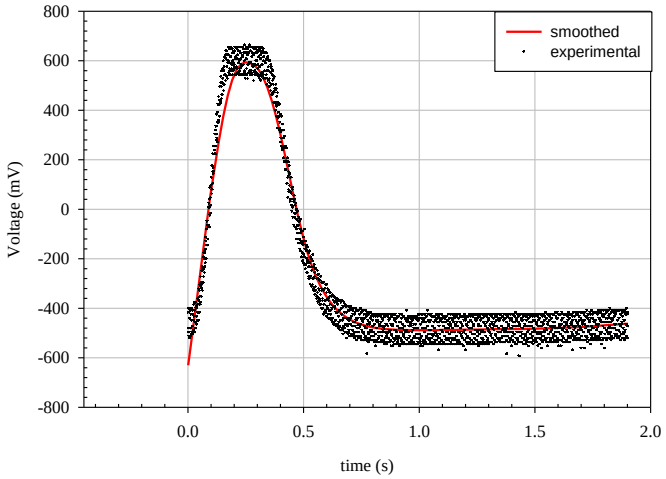

Figure 8. Vibration at 620Hz and heat at 0.5Hz voltage waveform for experimental data and smoothed data.

To better quantify the effect of heat and vibrations, other frequency spots that are interesting to observe is when the heat is at 1Hz and the vibrations are at 43Hz as shown in Figure 9. In this figure, when the experimental and smoothed data are plotted, a sinusoidal waveform is clearly visible riding the smoothed total data. The sinusoidal waveform riding on the larger waveform seems to show a relatively regular pattern in time, namely a frequency of 43Hz.This is the same frequency the heat is applied to the sample. The larger waveform, smoothed, shows a frequency of 1Hz. These results seemed to indicate that the vibrations and heat together can provide a better contribution to overall power.

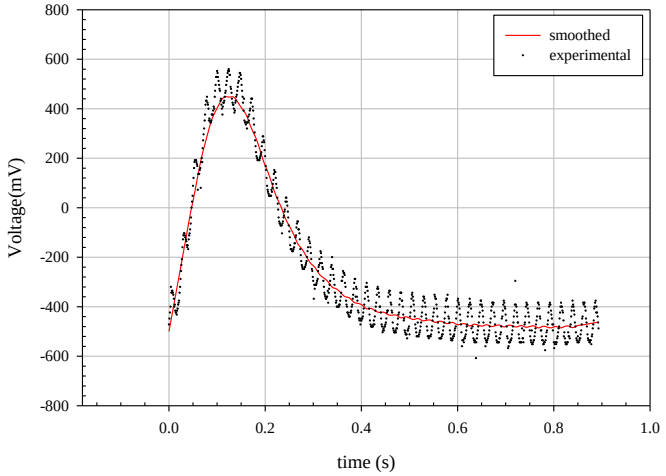

Figure 9. Heat and Vibrations (Heat at 1Hz and Vibrations at 43Hz).

The voltage produced with heat, vibrations, and both combined is accumulated using a commercially available energy harvesting circuit as described in the experimental setup. Typical curves during the charging are shown in Figure 10.

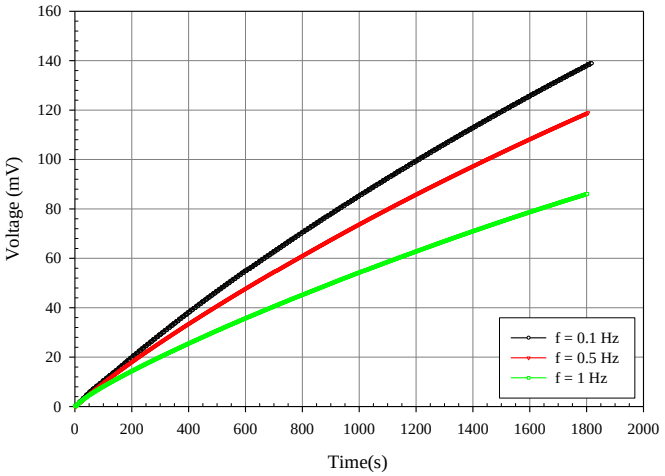

Figure 10. Typical charging curves with the heat cycling at different frequencies.

When vibrations and heat are coupled however, the charging of the energy harvesting circuit is different. In some cases, vibrations actually seem to be detrimental to the accumulated DC voltage. In others, vibrations seem to increase the rate of charging the circuit. These effects can be seen in Figure 11 for the case of heat at 0.1Hz and vibrations at four different frequencies. These results seem to indicate that there is an optimum value for both factors to contribute to harvesting energy.

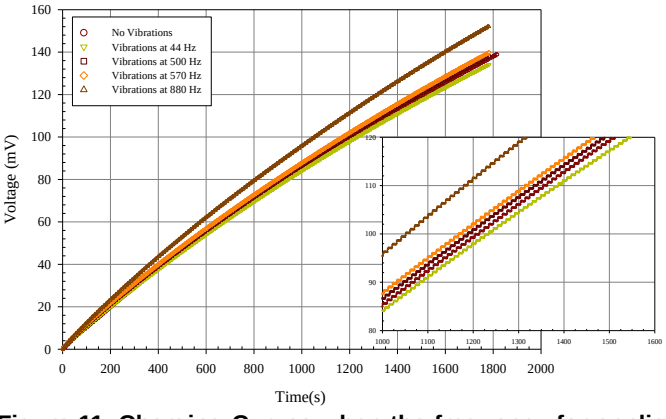

Figure 11. Charging Curves when the frequency for applied heating is at 0.1Hz and vibrations at different levels.

To provide a better understanding of the contributions due to heat and vibration and their significance to overall power, a two-way ANOVA of peak values of power accumulated on a 30min time span is performed. The factors to consider are many but the concentration of this statistical analysis is on the significance of the effect of heat and vibration and their interaction if any. The factors chosen are: applied heat (H1) and no vibrations (V0), case H1V0; no heat (H0) and applied vibrations (V1), case H0V1; applied heat (H1) and applied vibrations (V1), case H1V1. The results of the ANOVA are shown in Table 1.

Table 1. Two way ANOVA with interaction for heat and vibration cases.

Source of Variation	*SS*	*df*	*MS*	*F*	*P-value*	F_{crit}
Vibration	8.00	1	8.00	5.529	0.03663	4.75
Heat	70.79	1	70.79	48.898	0.00001	4.75
Interaction	7.52	1	7.52	5.194	0.04175	4.75
Within	17.37	12	1.45			
Total	103.68	15				

The results of the statistical analysis show that there is an interaction that is significant between cyclic heat and vibrations. This demonstrates that for some applications heat and vibrations could be coupled to optimize energy scavenging.

CONCLUSIONS

An energy scavenging feasibility study was conducted by investigating the pyroelectric and piezoelectric effects. This was accomplished by using energy from a heating lamp and energy from a vibrating beam. Both effects were investigated independently and coupled and were used to charge energy to a capacitor in the form of an energy harvesting circuit. Results showed that depending on the frequency of applied heat and applied vibrations, the scavenged energy varies. In some cases beam vibrations coupled with applied heating have a slightly negative effect on scavenged energy. In general, both effects if tuned properly may have a significant effect in overall accumulated power. Statistical analysis also confirms with a 95% confidence level that the interaction effect between heating and vibration is significant and should be taken into account when designing energy scavenging systems. It was determined that at the best tested parameters the rate of charge increases by approximately 12%.

ACKNOWLEDGMENTS

The authors would like to thank the School of Engineering of Virginia Commonwealth University and the Smart Materials Lab for their financial support.

REFERENCES

[1] IEEE Standard Definitions of Piezoelectric Terms (1986). *ANSI/IEEE 180-1986 IEEE*, New York.

[2] Jaffe, B., Cook W.R., and Jaffe, H. (1971). Piezoelectric Ceramics, *Academic Press LTD*, London.

[3] Piezoelectric Ceramics: Principles and Applications (2002). *APC International, Ltd*, Mackeyville, PA.

[4] Antaki, J., Bertocci, G., Green E.C., Nadeem A., Rintoul, T., Kormos, R.L., and Griffith, B. (1995). "A Gait Powered Autologous Battery Charging System For Artificial Organs", *ASAIO Journal*, (41): M588-M595.

[5] Bryant, R. G. (1996). "LaRC™-SI: a soluble aromatic polyimide", *High Performance Polymers*, (8) 607-615.

[6] Fay, J. A., and Golomb, D. S. (2002). "Energy and the Environment", *Oxford University Press*.

[7] Goldfarb, M., and Jones, L.D. (1999). "On the Efficiency of Electric Power Generation with Piezoelectric Ceramic", *Journal of Dynamic Systems, Measurement, and Control*. Vol. 121: 566-571.

[8] Umeda, M., Nakamura, K., and Ueda, S. (1996). "Analysis of the Transformation of Mechanical Energy to Electrical Energy Using Piezoelectric Vibrator", *Japanese Journal of Applied Physics – Part 1 Regular Papers and Short Notes*. Vol. 35, N.5 pt. B: 3267-3274.

[9] Roundy, S., Wright, P., Rabaey, J. (2004). "Energy Scavenging For Wireless Sensor Networks", *Kluwer Academic Publishers*.

[10] Sodano, H.A., Inman, D.J. and Park, G., (2005). Comparison of Piezoelectric Energy Harvesting Devices for Recharging Batteries, *Journal of Intelligent Material Systems and Structures*, v 16, n 10, p 799-807.

[11] Rowe, D.S. (1983). Modern Thermoelectrics, *Prentice Hall* p. 1-10.

[12] Sebald, G., Guyomar, D., Agbossou, A. (2009). "Smart Materials and Structures" v 18, n 12, p 125006 (7 pp.)

[13] Olsen, R.B., Bruno, D.A., Briscoe, J.M. (1985). "Pyroelectric conversion cycles", *Journal of Applied Physics*, vol.58, no.12, pp.4709-4716.

[14] Cuadras, A., Gasulla, M., Ghisla, A., and Ferrari, V., (2006). "Energy harvesting from PZT pyroelectric cells", *Instrumentation and Measurement Technology Conference*, pp.1688 – 1672.

[15] Sebald, G., Lefeuvre, E.,Guyomar, D., (2008). "Pyroelectric Energy Conversion: Optimization principles", *IEEE Transactions on Ultrasonics, Ferroelectrics, and Frequency Control*, v 55, n 3, p 538-551.

[16] Sebald, G., Guyomar, D., Agbossou, A. (2009). "On Thermoelectric and Pyroelectric Energy Harvesting", *Smart Materials and Structures*, v 18, n 12, p 125006 (7 pp.).

[17] Khodayari, A., Pruvost, S., Sebald, G., Guyomar, D., Mohammadi, S. (2009). "Nonlinear Pyroelectric Energy Harvesting From Relaxor Single Crystals", *IEEE Transactions on Ultrasonics, Ferroelectrics and Frequency Control*, v 56, n 4, p 693-9.

[18] Rashid M.H., (2001). Power electronics handbook, *Academic Press*, pp. 539–562.

[19] Ottman, G.K., Hofmann, H.F., Bhatt, A.C., and Lesieutre, G.A. (2002). "Adaptive Piezoelectric Energy Harvesting Circuit for Wireless Remote Power Supply", *IEEE Transactions on Power Electronics*, v 17, n 5, p 669-76.

[20] MFC-brochure, *Smart Material Corp.*, www.smart-material.com, 2010.

[21] EH300/EH301 EPAD Energy Harvesting Modules Brochure, *Advanced Linear Devices, Inc.*, www.aldinc.com, 2010.